

New approach for approximating the continuum wave function by Gaussian basis set

Marcelo Fiori ^{a,*}, J.E. Miraglia ^b

^a Departamento de Física, Facultad de Ciencias Exactas, Universidad Nacional de Salta, Salta, Argentina

^b Instituto de Astronomía y Física del Espacio, Consejo Nacional de Investigaciones Científicas y Técnicas, Departamento de Física, Facultad de Ciencias Exactas y Naturales, Universidad de Buenos Aires, Casilla de Correo 67, Sucursal 28, (C1428EGA) Buenos Aires, Argentina

ARTICLE INFO

Article history:

Received 28 December 2011
Received in revised form
15 June 2012
Accepted 9 July 2012
Available online 14 July 2012

Keywords:

Wave functions and integrals
Coulomb functions
Minimization and fitting
Ionization

ABSTRACT

A new approach for approximating the continuum wave functions for hydrogenic atoms with Gaussians basis sets is developed and tested. In this the plane wave is left unchanged and the distorting factor, represented by the Confluent Hypergeometric function, is expanded as a sum of Spherical Harmonics multiplied by a series of Gaussians. In this way the number of spherical waves and Gaussians will be significantly reduced and the plane wave will be responsible for the momentum conservation.

As compared with previous methods that expand the full continuum, including the plane wave, our strategy does not require a great quantity of partial waves for convergence. Dense oscillations which are characteristic of the plane wave, are avoided. To test the performance of this approximation to describe a free-bound atomic form factor, the ionization cross section of hydrogen by impact of protons in first Born approximation is calculated. Compared with the exact results, a good agreement with just 4 spherical waves and ten Gaussians each is obtained. The method looks very interesting, especially to speed up atomic and molecular collision calculations involving the continuum.

© 2012 Elsevier B.V. All rights reserved.

1. Introduction

Since the seminal work of Boys [1], the use of Gaussian Type Orbitals (GTOs) to describe atomic and molecular states has become a fundamental tool in quantum chemistry. It has been very successful in the calculation of ground as well as excited states. The greatest advantage of the GTOs over the Slater Type Orbitals (STOs) is their power to reduce multicenter integrals to a simple closed form [2–4]. This formidable reduction in computing time has displaced the STO from the mainstream of computing codes in Molecular Physics. The difference is still more favorable when dealing with traveling orbitals, i.e. integrals containing plane waves $\exp(i\mathbf{k} \cdot \mathbf{r})$. Thus, when using GTOs, a closed form for matrix elements integrals can be found; whereas numerical integrals are required when using STOs. Nevertheless, STOs are still very important in atomic collision calculations for several reasons: to properly describe the cusp condition, and to exactly represent the hydrogenic wave functions, among others. Several authors [5,6] have expanded the close coupling technique in order to solve the Schroedinger equation by using the GTO set since the matrix elements, including translation factors, can be evaluated analytically.

Even though there is much published literature on the use of GTOs in bound states, there is not much work about GTOs in continuum states. In the seventies, GTOs were used in *R*-matrix calculations as basis functions to study elastic collision of electrons with H_2 [7], and in cross sections for charge transfer in proton–hydrogen collisions at intermediate and high energies [5]. The UK *R*-Matrix group [8] based on the early work of Nestmann and Peyerimhoff [9,10] used the GTOs to represent continuum states. In these articles the authors optimized the GTO basis set by fitting radial wave functions (Bessel functions for neutral targets). Later a general procedure for generating such basis sets for both charged and neutral systems was developed by Faure et al. [11,12]. The aim of this procedure is to find the best set of Gaussian exponents that fit the continuum wave functions within an energy interval. With this set of exponents, any continuum wave function in that interval can be adjusted. Thus Tarana and Horacek [13] have calculated electron- F_2 elastic cross sections with *R*-Matrix using a continuum GTO basis set. They tested the quality of their basis set by solving the *R*-Matrix problem for the free particle where the phase shifts are zero.

Ref. [14] refers to another relevant method, which consists of a diagonalization of the Hamiltonian in a GTO set for a given set of eigenvalues. The basis obtained should describe the whole oscillatory behavior of the continuum.

All cited methods approximate the radial continuum functions using a series of Gaussians. For example, take the expansion of a

* Corresponding author. Tel.: +54 387 4255408; fax: +54 387 4255449.
E-mail address: marcelorfiori@gmail.com (M. Fiori).

free state represented by a plane wave:

$$\frac{e^{i\mathbf{k}\cdot\mathbf{r}}}{(2\pi)^{3/2}} = \sum_{lm} i^l \sqrt{\frac{2}{\pi}} j_l(kr) Y_l^m(\hat{\mathbf{k}}) Y_l^{m*}(\hat{\mathbf{r}}). \quad (1)$$

If the GTO set is used to represent the radial function, this basis would describe the oscillation of the $j_l(kr)$ Bessel function. Considering that one Gaussian function can represent at most one maximum or one minimum, we would need as many Gaussians as half-oscillations. If we have high energy electrons, (large values of k) a large number of Gaussians would be required.

In this article another approach will be used. In general, the continuum wave function can be written:

$$\psi_{\mathbf{k}}(\mathbf{r}) = \frac{e^{i\mathbf{k}\cdot\mathbf{r}}}{(2\pi)^{3/2}} D(\mathbf{k}, \mathbf{r}), \quad (2)$$

where $D(\mathbf{k}, \mathbf{r})$ is the distortion factor introduced by the potential. The aim of this work is to expand only the distorting factor $D(k, r)$ in a series of spherical functions of the form

$$D(\mathbf{k}, \mathbf{r}) = \sum_{l,m} D_l(k, r) Y_l^m(\hat{\mathbf{k}}) Y_l^{m*}(\hat{\mathbf{r}}) \quad (3)$$

and to approximate the radial functions $D_l(k, r)$ by a series of Gaussians. Thus, the plane wave in (2) representing the kinematical characteristic of the continuum is left intact.

We expect the factor $D(\mathbf{k}, \mathbf{r})$ to behave smoothly because the origin of the strong oscillatory pattern is mainly due to the plane wave, which is here excluded from the expansion. It is well-known that the plane waves are not a problem in the calculation of the integrals when Gaussians are used due to the fact that a closed form can be obtained.

In this article the factor $D(\mathbf{k}, \mathbf{r})$ for the Coulomb case will be expanded in Gaussians and the ionization cross section of hydrogen in the ground 1s-state by impact of protons will be calculated. This is a typical calculation in atomic collision involving the continuum. As the exact result is known [15–18] it will be feasible to examine the possibility of this method to describe not only integrated cross sections but also singly and doubly differential cross sections where the lack of precision is more evident.

In Section 2 the theoretical aspect and the matrix element calculation using Gaussians are introduced. In Section 3 the exact calculations are compared with the results obtained with the GTOs. Atomic units are used except where indicated.

2. The method

The continuum state of a hydrogenic atom can be expressed as follows

$$\psi_{\mathbf{k}}^-(\mathbf{r}) = \frac{e^{i\mathbf{k}\cdot\mathbf{r}}}{(2\pi)^{3/2}} D^-(a, \mathbf{k}, \mathbf{r}), \quad (4)$$

where $D^-(a, \mathbf{k}, \mathbf{r})$ is the Coulomb distortion to the plane wave due to the Coulomb potential satisfying the ingoing asymptotic condition

$$D^-(a, \mathbf{k}, \mathbf{r}) = N(a) {}_1F_1(-ia, 1, -i(kr + \mathbf{k} \cdot \mathbf{r})), \quad (5)$$

$N(a) = e^{\pi a/2} \Gamma(1 + ia)$ is the so-called Gamow factor $a = Z/k$, Z is the Coulomb nuclear charge and ${}_1F_1$ is the Confluent Hypergeometric function. Starting with the integral representation of ${}_1F_1$ (Eq. (6.5.1) in Ref. [19]), and after a complex algebraic calculation which is omitted here, the following expansion is obtained:

$$D^-(a, \mathbf{k}, \mathbf{r}) = \sum_{lm} D_l^-(a, r, k) y_l^m(\hat{\mathbf{k}}, \hat{\mathbf{r}}), \quad (6)$$

$$y_l^m(\hat{\mathbf{k}}, \hat{\mathbf{r}}) = k^l Y_l^m(\hat{\mathbf{k}}) r^l Y_l^{m*}(\hat{\mathbf{r}}), \quad (7)$$

and

$$D_l^-(a, r, k) = N(a) 4\pi \frac{\Gamma(l - ia)(-i)^l}{\Gamma(-ia)l!(2l + 1)!!} \times {}_1F_1(l - ia, 2l + 2, -2ikr). \quad (8)$$

The core aim of this method is to approximate $D_l^-(a, r, k)$ (real and imaginary part) with a sum of Gaussians

$$D_l^-(a, r, k) \cong \sum_s a_{ls}(k) e^{-\alpha_{ls} r^2}. \quad (9)$$

The success of this method depends on two assumptions: First, a rapid convergence with l in Eq. (6) is required. It will be proved that a good approximation will be obtained with few partial waves; it will suffice to accurately describe the magnitudes of interest considering $l_{\max} = 8$. Second, if $D_l^-(a, r, k)$ does not have a strong oscillatory pattern, the expansion (9) works with a small number of Gaussians. It is expected that the plane wave, which has been removed from the expansion, will take away most of the oscillatory patterns of the continuum.

It must be remembered that, in the conventional treatment, the expansion in partial waves is:

$$\psi_{\mathbf{k}}^-(\mathbf{r}) = 4\pi \sum_{lm} i^l \frac{u_l(r)}{kr} Y_l^m(\hat{\mathbf{k}}) Y(\hat{\mathbf{r}})$$

where function $u_l(r)$ is real [17]; while this function $D_l^-(a, r, k)$ is complex and both the real and the imaginary parts must be approximated separately. But this fact is greatly compensated for by the diminution in the necessary number of Gaussian basis functions and the reduction of partial waves required.

To find the best parameter set of Eq. (9), strategies similar to the one used in Refs. [11,9] are followed. First, a bidimensional grid on k and r is established. Then a grid of equally spaced values of k so that $k_{\mu} = 0.1 + 1.2(\mu - 1)$ a.u. with μ ranging from 1 to 12 is chosen, together with another set of r_{ν} with ν ranging from 1 to 120 in a constant mesh, so that the range of r -values lie in the interval [0, 14] a.u. It is assumed that the set of Gaussian coefficients α_{nl} for a given value of angular momentum holds for all values chosen for k . In this bidimensional grid the distance function is built

$$F_l(\alpha_{l1} \dots \alpha_{lS}) = \sum_{\mu} \frac{\sum_{\nu} \left| \sum_s a_{ls\mu} e^{-\alpha_{ls} r_{\nu}^2} - D_{lv\mu} \right|^2}{\sum_{\nu'} |D_{lv'\mu}|^2} - \sum_{i=2}^S \sum_{j=1}^{i-1} \exp\left(-g \left| \frac{\alpha_{li}}{\alpha_{lj}} - \frac{\alpha_{lj}}{\alpha_{li}} \right| \right), \quad (10)$$

where for sake of simplicity, it was shortened $D_{lv\mu} = D_l^-(a, r_{\nu}, k_{\mu})$, and $a_{ls\mu} = a_{ls}(k_{\mu})$. The exact values of the Hypergeometric function included in $D_{lv\mu}$ were evaluated with the Perger et al. [20] code. The second term in Eq. (10) is added to avoid the convergence of two different α_{ls} in the same value [9]. The strength of this separation has been set to be $g = 20$.

The values of k_{μ} here considered cover a wide spectrum of electron energies, which allows the study of the ionization of hydrogen atoms for impact energies between few keV to 2 MeV/amu. To obtain the set of α_{ls} , Eq. (10) is minimized and the coefficients $a_{ls\mu}$ were found by a least-square fit to the set $D_{lv\mu}$. The minimum of $F_l(\alpha_1 \dots \alpha_N)$ was obtained by the Powell method using $\ln \alpha_{ls}$ as variational parameters [21,11]. A list of α_{ls} for the first eight values of angular momentum for hydrogen ($Z = 1$) are given in the Tables 1 and 2 for real and imaginary parts of the functions, respectively. For other nuclear charges ($Z > 1$) the same coefficients with an appropriate scaling can be used. In atomic units the transformation required is to replace r by $\frac{r}{Z}$, and it is due to the scaling symmetry of the Schroedinger equation for the Coulomb potential [22].

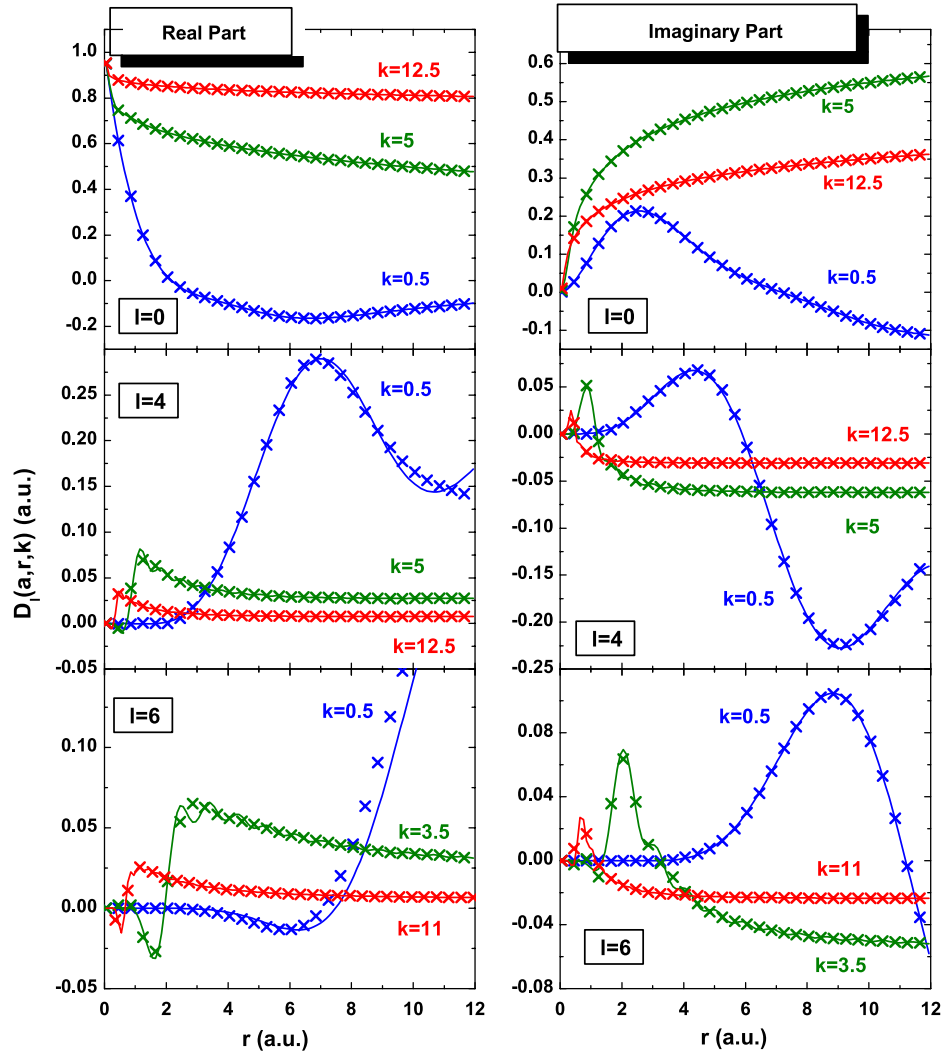


Fig. 1. Functions $D_l^-(a, r, k)$ as a function of r for three values of angular momenta, $l = 0$, $l = 4$ and $l = 6$ and three values of k as indicated. Solid lines: exact results given by Eq. (7), crosses: our 10-Gaussian approximation given by Eq. (8).

Table 1

Exponents of the continuum basis set α_{ls} given by Eq. (8). Real part.

i	$l = 0$	$l = 1$	$l = 2$	$l = 3$	$l = 4$	$l = 5$	$l = 6$	$l = 7$	$l = 8$
1	50.14027	5.480120	6.150530	4.104476	2.788807	2.0578627	2.516662	1.166146	1.562035
2	7.052100	3.240182	3.809258	2.741133	1.909801	1.4572600	1.765046	0.842100	1.123037
3	2.025116	1.931101	2.375013	1.854451	1.276196	1.0283147	1.236053	0.592876	0.791875
4	1.082984	1.143770	1.465699	1.252529	0.668160	0.7095468	0.845401	0.379052	0.446408
5	0.278845	0.664955	0.891287	0.839097	0.278582	0.4734297	0.565162	0.246379	0.280483
6	0.149681	0.163297	0.381556	0.554004	0.123669	0.1787970	0.291030	0.166075	0.189987
7	0.081580	0.093433	0.105105	0.231613	0.080425	0.1143517	0.144526	0.111321	0.133231
8	0.045299	0.052503	0.056098	0.071236	0.051125	0.0749643	0.099716	0.072590	0.092780
9	0.009268	0.020868	0.024499	0.041493	0.031927	0.0399839	0.069167	0.045661	0.064255
10	0.000100	0.002373	0.003576	0.010153	0.009945	0.0188267	0.021568	0.011987	0.037582

2.1. Approximate wave functions

With the coefficients obtained, any wave functions ranging near the k -interval used to calculate the coefficients can be approximated using a simple least square fit. Fig. 1 plots the exact value of the real and imaginary part of $D_l^-(a, r, k)$ given by Eqs. (8) in solid lines, along with our approximated values given by the expansion (9) for three values of angular momenta ($l = 0$, $l = 4$ and $l = 6$) represented by crosses. In this figure we can observe the deterioration level of the Gaussian expansion with the angular

momentum. For $l = 0$ the expansion is very good for the range of energy considered. For larger values of l the exact value of $D_l^-(a, r, k)$ presents fine oscillations that this 10-Gaussian expansion cannot fully reproduce. Nevertheless, it is still true that for $l = 6$, this approximation does not deviate significantly from the exact values.

Fig. 2 plots the total solution of the wave equation $\psi_{\mathbf{k}}^-(\mathbf{r})$ for the hydrogen for four values of k and ejected electron angles θ with respect to \mathbf{k} . In this last case the series (6) are approximated with $l_{\max} = 8$. The agreement is quite good even at small distances

Table 2
Exponents of the continuum basis set α_{ls} given by Eq. (8). Imaginary part.

i	$l = 0$	$l = 1$	$l = 2$	$l = 3$	$l = 4$	$l = 5$	$l = 6$	$l = 7$	$l = 8$
1	6.207101	11.81367	4.443446	2.702729	1.799427	1.875402	1.928604	1.202149	1.134437
2	1.791078	2.964620	2.630378	1.765517	1.230155	1.309149	1.346854	0.875973	0.829470
3	0.476867	1.385471	1.548170	1.116467	0.808150	0.883093	0.935386	0.503411	0.592771
4	0.264939	0.815529	0.940160	0.643399	0.451763	0.544773	0.641143	0.246747	0.391066
5	0.147263	0.388077	0.581966	0.242294	0.147394	0.339040	0.430836	0.170105	0.216914
6	0.081249	0.106435	0.223086	0.152682	0.094082	0.104770	0.232519	0.117861	0.149721
7	0.044104	0.053218	0.055032	0.096328	0.060544	0.071043	0.087134	0.080035	0.104061
8	0.023261	0.029464	0.034161	0.059423	0.038126	0.047928	0.059904	0.053185	0.069528
9	0.011612	0.015722	0.020773	0.036466	0.023444	0.031745	0.040492	0.034412	0.045327
10	0.000299	0.008701	1.64×10^{-9}	0.008813	0.013295	0.020367	0.015147	0.020911	0.019565

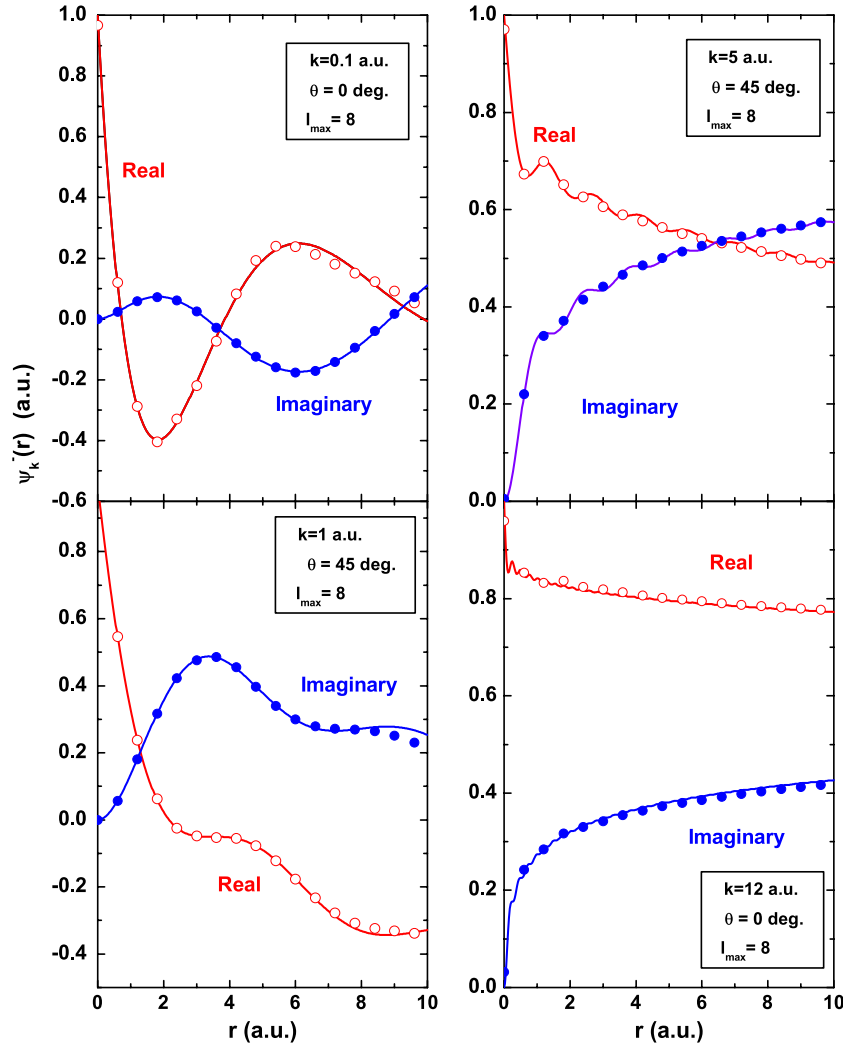


Fig. 2. Real and imaginary part of the continuum wave functions $\psi_k^-(\mathbf{r})$ for different values of k and ejected angles $\cos \theta = \hat{\mathbf{k}} \cdot \hat{\mathbf{r}}$ as indicated. Solid lines: exact results given by Eqs. (3) and (4), dots: Gaussian approximation given by Eqs. (3), (5) and (8) with 10 Gaussians and $l_{\max} = 8$.

where the main contribution to the matrix elements is relevant. It is then concluded that our strategy to approximate the wave function is adequate. In the next section, its ability to approximate the free-bound matrix elements will be considered.

3. Ionization of hydrogen

The first Born approximation for hydrogen ionization by protons using this Gaussian expansion is calculated. Its transition matrix element is denoted by

$$T_{ik} = -\frac{4\pi Z_p}{q^2} F_{ik}(\mathbf{q}), \quad (11)$$

$$F_{ik}(\mathbf{q}) = \int d\mathbf{r} \psi_k^{-*}(\mathbf{r}) e^{i\mathbf{q}\cdot\mathbf{r}} \psi_i(\mathbf{r}), \quad (12)$$

where $F_{if}(\mathbf{q})$ is the atomic form factor, Z_p is the projectile Coulomb charge and \mathbf{q} is the momentum transfer vector. If the continuum wave function denoted by Eq. (5) and the exact ground state of hydrogen are used, Eq. (12) has an analytical solution in [15,16].

To exploit this Gaussian scheme, it is required that ψ_i is also expanded in Gaussians. When dealing with the 1s-ground state ($i = 1s$), just a six term expansion is used,

$$\psi_{1s}(\mathbf{r}) \cong \sum_{t=1}^6 b_{0t} e^{-\beta_{0t} r^2}, \quad (13)$$

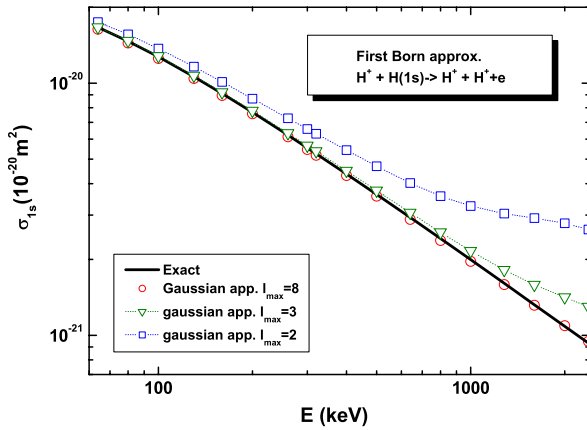


Fig. 3. Total ionization cross section of hydrogen by the impact of protons as a function of the projectile energy calculated with the first Born approximation. Solid line: exact calculation. Symbols connected with dotted lines: Gaussian expansion with $l_{\max} = 2$ (empty squares), 3 (empty triangles), and 8 (empty circles), as indicated.

where the coefficients b_{0t} and β_{0t} are found to be

$$\beta_{0t} = (0.33741, 0.21597, 0.20636, 0.16089, 0.07044, 0.00892) \text{ and}$$

$$\beta_{0t} = (7.88373, 1.42466, 0.55364, 0.24547, 0.11424, 0.05347).$$

The form factor then can be denoted as

$$F_{1s\mathbf{k}}(\mathbf{q}) = \sum_{lm} \sum_{s\ t} b_{0t} a_{ls}(k) k^l Y_{l,m}(\hat{\mathbf{k}}) \times \int d\mathbf{r} r^l Y_{l,m}(\hat{\mathbf{r}}) e^{-\alpha_{ls} r^2} e^{i\mathbf{Q}\cdot\mathbf{r}} e^{-\beta_{0t} r^2} \quad (14)$$

with $\mathbf{Q} = \mathbf{q} - \mathbf{k}$. Due to the rectangular symmetry of the Gaussians, it is convenient to turn the *Spherical Harmonics* $Y_{l,m}(\hat{\mathbf{r}})$ into the

Cartesian form using the relation

$$r^l Y_{l,m}(\hat{\mathbf{r}}) = \left[\frac{(l-m)!}{(l+m)!} \right]^{\frac{1}{2}} \sum_{k=0}^{\frac{l-m}{2}} C_1(l, m, k) \times \sum_{p=0}^m C_2(m, p) \sum_{i=0}^k \sum_{j=0}^{k-i} \binom{k}{i} \binom{k-i}{j} \times x^{2(k-i-j)+p} y^{2j+m-p} z^{2i+l-2k-m}, \quad (15)$$

$$C_1(l, m, k) = \frac{(-1)^k}{2^l} \binom{l}{k} \binom{2l-2k}{l} \frac{(l-2k)!}{(l-2k-m)!}, \quad (16)$$

$$C_2(m, p) = \binom{m}{p} (\cos \delta + i \sin \delta), \quad (17)$$

and $\delta = (m-p)\pi/2$. In this way the atomic form factor can be expanded in a sum of three-dimensional integrals, which can be denoted as a product of three independent integrals (on x , y and z) of type

$$\int e^{iQ_x x} e^{-ax^2} x^n dx = n! e^{-\frac{Q^2}{4a}} \sqrt{\frac{\pi}{a}} i^n \left(\frac{Q}{2a}\right)^n \times \sum_{s=0}^{\frac{n}{2}} \frac{(-1)^s}{(n-2s)!} \left(\frac{a}{Q^2}\right)^s. \quad (18)$$

The atomic form factor then has a closed form in terms of the Gaussian set of the continuum, keeping its main characteristic, which is the plane wave, intact.

3.1. Result

Cross sections for ionization of hydrogen are

$$\sigma_{1s} = \int dE \int d\Omega \frac{d\sigma_{1s,\mathbf{k}}}{dE d\Omega}, \quad (19)$$

$$= \int dE \frac{d\sigma_{1s,\mathbf{k}}}{dE} = \int d\Omega \frac{d\sigma_{1s,\mathbf{k}}}{d\Omega}, \quad (20)$$

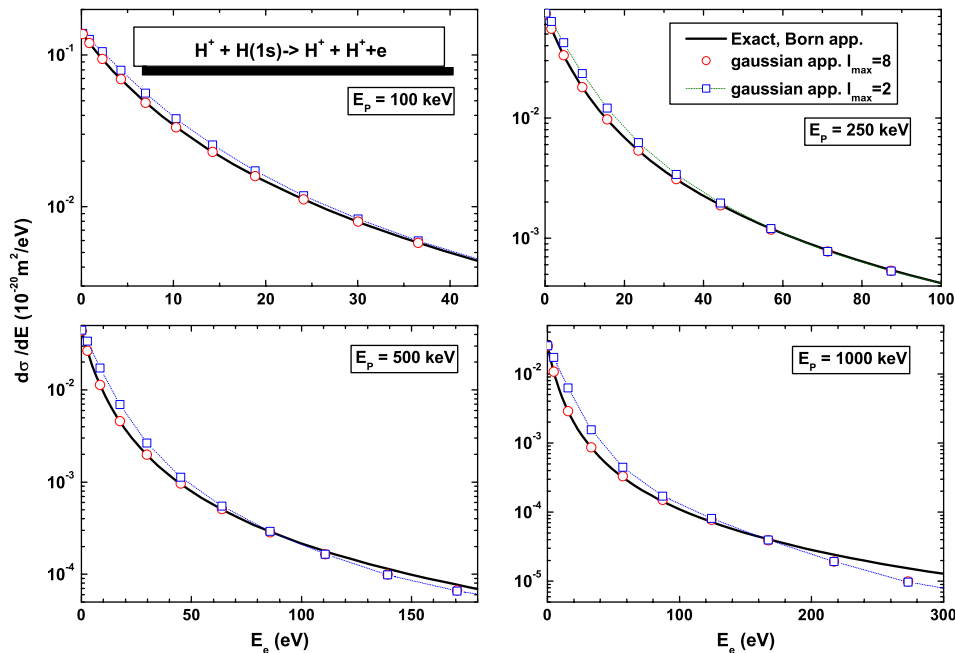


Fig. 4. Single differential cross section for ionization of hydrogen as a function of the electron energy calculated in first Born approximation. Solid lines: Exact result. Red empty circles: Gaussian approximation with $l_{\max} = 8$. Blue empty squares: Gaussian approximation with $l_{\max} = 2$. (For interpretation of the references to colour in this figure legend, the reader is referred to the web version of this article.)

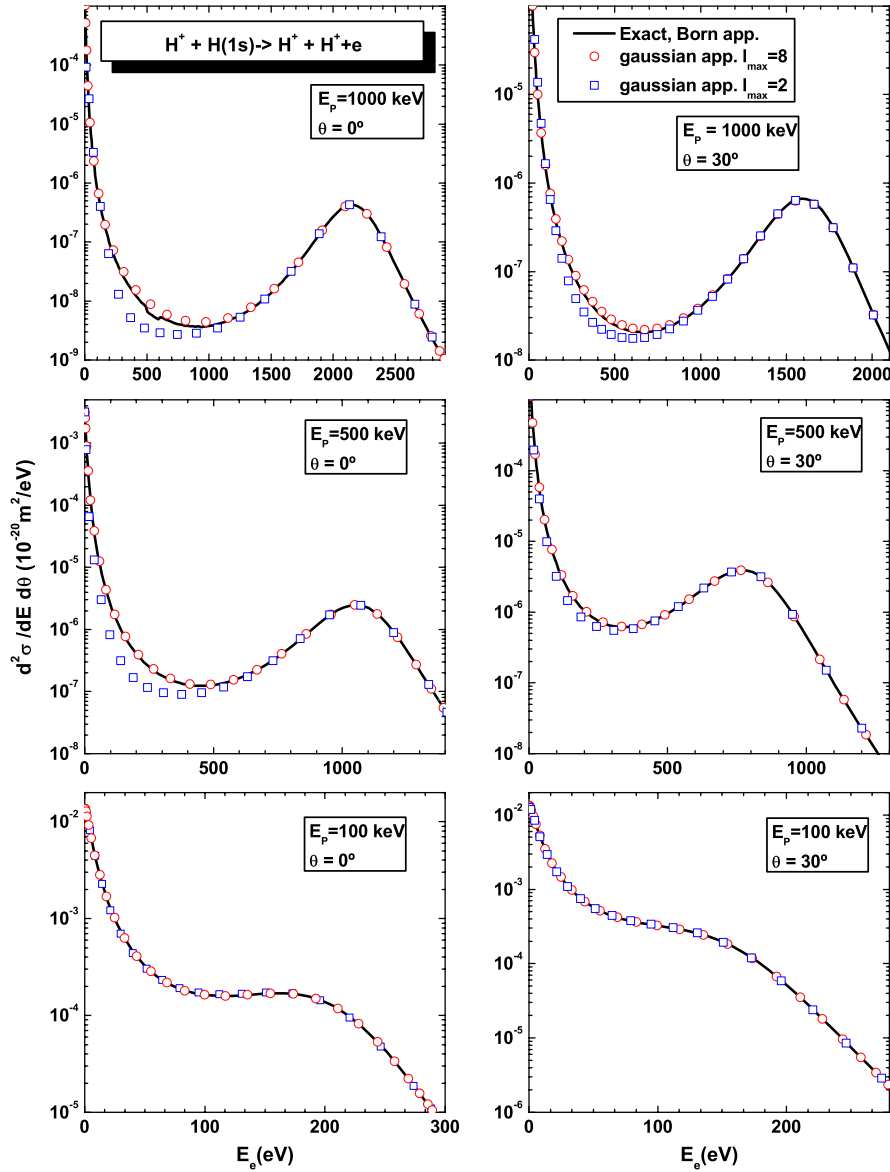


Fig. 5. Double differential cross section for ionization of hydrogen as a function of the electron energy for different ejection angles calculated in first Born approximation. Solid lines: Exact result. Red empty circles: Gaussian approximation with $l_{\max} = 8$, and blue empty circles the same with $l_{\max} = 2$. (For interpretation of the references to colour in this figure legend, the reader is referred to the web version of this article.)

$$\frac{d\sigma_{1s,\mathbf{k}}}{dE d\Omega} = \frac{(2\pi)^4}{v^2} \int d\eta |T_{1s,\mathbf{k}}|^2, \quad (21)$$

where $E = k^2/2$ is the electron energy, Ω is the solid angle of emission, and η is the bidimensional transversal momentum transfer.

To begin with, the total cross section is examined. Fig. 3, plots σ_{1s} as a function of the proton impact energy. As indicated in the previous section, ten values of α_{1s} (see the table), $l_{\max} = 2, 3$ and $8, 10$ Gaussians for each value of k and l (a_{1s} in Eq. (9)), and 12 values of k for a Gaussian integration are used. The exact first Born results [18] using the full hypergeometric functions are indicated by a solid black line. The agreement between this Gaussian expansion and the exact first Born results is very good. By using a moderate expansion, only $l_{\max} = 3$, a reasonable result is achieved up to 1 MeV protons. Even with a short expansion, $l_{\max} = 2$, a regular performance at low impact energies is obtained. We can then extract the following relation between the impact energy and the l_{\max} ; the larger the projectile energy, the larger l_{\max} .

The test can be progressed to explore the single differential cross section. Fig. 4 shows $d\sigma_{1s}/dE$ as a function of E for four different proton impact energies, 100, 250, 500 and 1000 keV. Results with $l_{\max} = 3$ are difficult to distinguish from the ones of $l_{\max} = 8$. The agreement is very good and reasonable values using $l_{\max} = 2$ can be obtained.

The binary cusp is correctly described in every case, and this is mainly due to the fact that the plane wave $e^{i\mathbf{k}\cdot\mathbf{r}}$ in the wave function is maintained. Also, by reducing l_{\max} the soft electron energy region is deteriorated and this region is the one that contributes the most to the total cross section. That is the origin of the failure of the simple expansion with $l_{\max} = 2$ observed in Fig. 3.

The most complex test is the double differential cross section. Fig. 5 displays $d\sigma_{1s}/dEd\Omega$ as a function of the ejected electron energy for two escaping angles $\theta = 0$ and 30° and for three impact energies: 100, 500 and 1000 keV. In this figure a black line shows the exact result of Ref. [18], and red (blue) empty circles the Gaussian results with $l_{\max} = 8$ ($l_{\max} = 2$). The agreement with the exact calculation (represented by the black line) is quite good. This

method is capable of reproducing the binary peak at $E \sim 200$ eV for $E_p = 100$ keV, $E \sim 1050$ eV for $E_p = 500$ keV and $E \sim 2100$ for $E_p = 1000$ keV, in the forward direction ($\theta = 0^\circ$). The binary peak is also well-reproduced for the angle of $\theta = 30^\circ$. The explanation is simple: as the full plane wave in the wave function is maintained, the momentum conservation is accurately described and, consequently, the binary sphere is correctly reproduced. Here it should be noted that for the correct description of the binary peak in a conventional (full) partial wave expansion as many as 30 partial waves are necessary for the energies considered here. Not only is the binary peak region well reproduced but also the soft peak region where the total cross section is more sensitive. In the intermediate energies there are some small discrepancies in the calculations with $l_{\max} = 8$ and a larger for $l_{\max} = 2$ for projectile impacts of 500 and 1000 keV. For lower energies the agreement is quite good regardless of the l_{\max} considered.

4. Conclusions

In this paper an alternative technique for approximating atomic continuum wave functions with a Gaussian basis is introduced. The procedure employed is based on the approximation of the distorting factor of the wave function (the Hypergeometric for the Coulomb case) leaving the plane wave intact. Although both, the real and imaginary parts of the function are approximated, this method allows the achievement a rapid convergence in partial waves and also a reduction in the number of Gaussians used to approximate the Hypergeometric function.

These approximate functions are used to calculate several cross sections in the ionization of hydrogen in the first Born approximation. Very good results are achieved when compared with the exact ones. The calculation has been adapted in order to use Cartesian coordinates. These coordinates are much more suitable for use in quantum chemistry for complex targets such as molecules or solids [4]. As the hydrogenic target has been used, $D_l^-(a, r, k)$ has a closed-form and the test is direct.

The expansion of these methods to more complex targets is work still outstanding. Although the methods used have been applied to the calculation of the hydrogen atom; they can also be implemented with other atoms containing more electrons, to do this, approximating the multielectron potential by a central potential is required. This can be done with several methods such as the OPM method [23]. In this case the function $D_l^-(a, r, k)$

is obtained by solving a differential equation and approximating the solutions by Gaussians in the same way as it is done with the hydrogenic case. Both the Gaussian approximation of the waves functions and the Cartesian coordinates calculus methods provide the necessary elements to calculate several cross sections of more complex targets as molecules in the Born approximation. The extension of this method to molecular targets is forthcoming work as well as the expansion of the methods beyond the Born approximation (i.e. Distorted Wave approximations).

Acknowledgments

The authors are grateful to Vicky Bertorelli, Soledad Loutaif and Juan Aparicio for critical reading of the manuscript.

References

- [1] S.F. Boys, Proc. R. Soc. Lond. Ser. A 200 (1950) 542.
- [2] W. Hehre, L. Radom, P.V. Scheleyer, J. Pople, AB Initio Molecular Orbital Theory, Wiley-Interscience, 1986.
- [3] F. Jensen, Introduction to Computational Chemistry, second ed., Wiley, 2006.
- [4] A. Szabo, N. Ostlund, Modern Quantum Chemistry: Introduction to Advanced Electronic Structure Theory, Dover, New York, 1996.
- [5] N. Toshima, J. Phys. B: At. Mol. Opt. Phys. 25 (1992) L635; N. Toshima, Phys. Rev. A 59 (1999) 1981.
- [6] L.F. Errea, L. Mendez, A. Riera, J. Phys. B: At. Mol. Opt. Phys. 12 (1979) 69.
- [7] Barry I. Schneider, Phys. Rev. A 11 (1975) 1957.
- [8] L.A. Morgan, J. Tennyson, C.J. Gillan, Comput. Phys. Comm. 114 (1998) 120.
- [9] B.M. Nestmann, S.D. Peyerimhoff, J. Phys. B: At. Mol. Opt. Phys. 23 (1990) L773.
- [10] B.M. Nestmann, R.K. Nesbet, S.D. Peyerimhoff, J. Phys. B: At. Mol. Opt. Phys. 24 (1991) 5133.
- [11] A. Faure, J.D. Gorfinkiel, L.A. Morgan, J. Tennyson, Comput. Phys. Comm. 144 (2002) 224.
- [12] J. Tennyson, Phys. Rep. 491 (2010) 29.
- [13] M. Tarana, J. Horacek, J. Chem. Phys. 127 (2007) 154319.
- [14] K. Kaufmann, W. Baumeister, M. Jungen, J. Phys. B: At. Mol. Opt. Phys. 22 (1989) 2223.
- [15] A. Nordsieck, Phys. Rev. 93 (1954) 785.
- [16] M.S. Gravielle, J.E. Miraglia, Comput. Phys. Comm. 69 (1992) 53.
- [17] M.R.C. Mc Dowell, J.P. Coleman, Introduction to the Theory of Ion-Atom Collisions, North Holland, Amsterdam, London, 1970.
- [18] D.S. Crothers, M. McCartney, Comput. Phys. Comm. 72 (1992) 288.
- [19] A. Erdelyi, W. Magnus, F. Oberhettinger, F.G. Tricomi, Higher Transcendental Functions, Bateman Manuscript Project, McGraw-Hill, 1953.
- [20] W.F. Perger, A. Bhalla, M. Nardin, Comput. Phys. Comm. 77 (1993) 249.
- [21] W.H. Press, B.P. Flannery, S.A. Teukolsky, W.T. Vetterling, Numerical Recipes in Fortran: The Art of Scientific Computing, second ed., Cambridge University Press, 1992.
- [22] Kurt Gottfried, Tung-Mow Yan, Quantum Mechanics: Fundamentals, second ed., Springer, 2003.
- [23] J.D. Talman, Comput. Phys. Comm. 54 (1989) 84.